Optical transmission spectra in quasiperiodic multilayered photonic structure

2006 J. Phys.: Condens. Matter 18 8737

(http://iopscience.iop.org/0953-8984/18/39/006)

Institute of Physics Publishing Journal of Physics: Condensed Matter

J. Phys.: Condens. Matter **18** (2006) 8737–8747 doi:10.1088/0953-8984/18/39/006

Optical transmission spectra in quasiperiodic multilayered photonic structure

F F de Medeiros[1], **E L Albuquerque**[1,2] **and M S Vasconcelos**[3]

[1] Departamento de Física, Universidade Federal do Rio Grande do Norte, 59072-970 Natal-RN, Brazil
[2] Center for Polymer Studies and Department of Physics, Boston University, Boston, MA 02215-2521, USA
[3] Departamento de Ciências Exatas, Centro Federal de Educação Tecnológica do Maranhão, 65025-001 São Luís-MA, Brazil

Received 31 July 2006, in final form 24 August 2006
Published 11 September 2006
Online at stacks.iop.org/JPhysCM/18/8737

Abstract
Optical transmission spectra in quasiperiodic multilayered photonic structures, composed of both positive (SiO_2) and negative refractive index materials, are calculated by using a theoretical model based on the transfer matrix approach for normal incidence geometry. The quasiperiodic structures are substitutional sequences, characterized by the nature of their Fourier spectrum, which can be dense pure point (e.g. Fibonacci sequence) or singular continuous (e.g. Thue–Morse and double-period sequences). The transmission spectra for the case where both refractive indices can be approximated by a different constant show a unique mirror symmetrical profile, with no counterpart for the positive refractive index case, as well as a striking self-similar behaviour related to the Fibonacci sequence. For a more realistic frequency-dependent refractive index, the transmission spectra are characterized by a rich transmission profile of Bragg peaks with no more self-similarity or mirror symmetry.

1. Introduction

Materials simultaneously possessing negative magnetic permeability and electric permittivity are physically permissible and would exhibit a negative refractive index [1]. They were coined as left-handed materials (LHM) because they support backward waves, for which the electric field $\vec{E}$, the magnetic field $\vec{H}$, and the Poynting vector $\vec{S}$ form a left-handed triplet. Besides, the group velocity of wave propagation in such media is opposite to its phase velocity, making the perfect lens possible (for an up-to-date review, see [2]).

Interest in LHM has been revived since 1999 onwards, when an artificial dielectric slab was designed and verified in experiments to exhibit negative material parameters, giving rise to a negative effective refractive index at microwave frequencies [3–5]. These unusual artificial media, which we shall refer to as metamaterials, are designed to possess simultaneously negative permittivity ϵ and permeability μ, respectively, in the same frequency region. However, a rigorously defined negative refractive index may not necessarily be a prerequisite for negative refraction phenomena. An alternative approach to attaining negative refraction uses the properties of *photonic crystals*, materials that lie on the transition between a metamaterial and an ordinary structured dielectric [6]. Their potential applications in high-technology industries have been responsible for the drive for fabrication of theses materials. For instance, due to their potential for negative reflection, it is possible to fabricate lenses with exotic optical properties, like optical images of objects that are smaller than the wavelenght of visible light (such as DNA molecules, proteins, etc). With the development of these superlenses [7], it is possible to realize photo-nanolithography, which would make smaller electronic device and circuits, resulting in more powerful computers [8]. Other applications are related to the development of new types of antennae, computer components and consumer electronics, such as cell phones, which use light instead of electricity for carrying signals and processing information, resulting in faster and cheaper communications [9].

To date, there are many methods for fabricating materials with negative refraction index. The first one was proposed by Pendry [3, 7, 10] by using conducting wires and loops, suspended in a dielectric substrate. While the wires assume an effective negative dielectric constant, the various loops provide a negative permeability in the same frequency band [5, 11]. Another method uses a two-dimensional photonic crystal [12–15], a medium with an in-plane periodic modulation of the dielectric constant, which, under proper conditions, can act as an effective medium with an homogeneous negative refractive index. A more recent method was proposed by Shalaev *et al* [16], by constructing a periodic array of nanorod pairs on a glass substrate fabricated using electron-beam lithography. Normally incident light, with an electric field polarized along the rods and a magnetic field perpendicular to the pair, takes on resonant behaviour due to the dielectric–metallic architecture. Above the resonant frequency, the circular current in the pair of rods can lead to a magnetic field opposing the external magnetic field of the light. The excitation of the plasmons causes resonance for the electric light component, while the magnetic fields generated by the circular current in the pair of rods causes a resonance for the magnetic light component, resulting in a resonant behaviour of the refractive index, which can become negative above the resonance (for a review, see [17]).

Periodic multilayered structures containing negative refractive index materials can be considered as a sequence of perfect lenses with unique transmittance or reflectance properties in the Bragg regime [18]. More recently, it has been shown that a one-dimensional periodic stack of layers with alternating dielectric and negative refractive index material, with zero averaged refractive index, displays a narrow spectral gap in the transmission, which is quite different from a Bragg reflection gap [19].

On the other hand, the discovery of quasiperiodic structures has fired up a new field of condensed-matter physics, giving rise to many practical applications (for an up-to-date review of this field, see [20]). For example, the multiwavelength second-harmonic generation [21] and the direct third-harmonic generation [22] have been realized in a Fibonacci superlattice. In the field of photonic crystals, an absolute photonic band gap in a 12-fold triangle–square tiling has recently been reported [23]. For quasiperiodic dielectric multilayers, Vasconcelos *et al* have shown the fractality of their optical spectra [24, 25], as well as the influence of the oblique incidence.

It is the aim of this work to investigate the transmission spectra of a light beam normally incident from a transparent medium into a multilayer photonic structure composed of SiO_2/metamaterial layers arranged in a quasiperiodical fashion, which follows the Fibonacci (FB), Thue–Morse (TM) and double-period (DP) substitutional sequences. Let us briefly review the types of quasiperiodic systems considered in this work. First we recall the definition

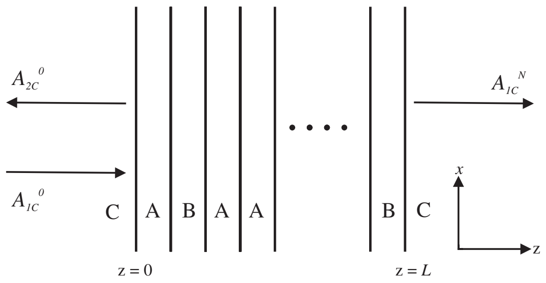

Figure 1. Schematic representation showing the geometry of the Fibonacci quasiperiodic multilayer system considered in this work. Here, L is the size of the whole superlattice structure.

of a *substitution sequence*. Take a finite set ξ (here $\xi = \{A, B\}$) called an *alphabet* and denote by ξ^* the set of all finitely long words that can be written in this alphabet. Now let ζ be a map from ξ to ξ^* by specifying that ζ acts on a word by substituting each letter (e.g. A) of this word by its corresponding image $\zeta(A)$. A sequence is then called a *substitution sequence*, if it is a fixed point of ζ, i.e. if it remains invariant if each letter in the sequence is replaced by its image under ζ. As examples of substitution sequences that have attracted the most attention in physics, we have (all with $\xi = \{A, B\}$): (a) the Fibonacci (FB) sequence, where the substitution rule is $A \rightarrow \zeta(A) = AB$, $B \rightarrow \zeta(B) = A$; (b) the Thue–Morse (TM) sequence, with the rule where $A \rightarrow \zeta(A) = AB$, $B \rightarrow \zeta(B) = BA$; (c) the double-period (DP) sequence, where $A \rightarrow \zeta(A) = AB$, $B \rightarrow \zeta(B) = AA$.

Although several theoretical techniques have been used to study the transmission spectra in these structures, in the present work we make use of the transfer matrix approach to analyse them, simplifying the algebra which would otherwise be quite involved (for a review, see [26]). Our main aim is the investigation of the behaviour of the light when it pass through the layered system, where medium B is fulfilled by a metamaterial and is characterized by a negative refraction index n_B.

The outline of this paper is as follows. In the next section, we present the theoretical calculation of the transmission spectra, which is based on the transfer-matrix approach. The numerical results for these spectra are shown in section 3, including a discussion about their main features. The conclusions are summarized in section 4.

2. Transfer matrix

We now intend to investigate the light transmission spectra in artificial structures exhibiting deterministic disorders, i.e. the Fibonacci, Thue–Morse and double-period superlattices. To calculate the light transmission rate through the multilayer system, we use a transfer-matrix approach for the electromagnetic fields. To this end, we consider that p-polarized (transverse electric, TE, wave) light of frequency ω is normally incident from a transparent medium C with respect to the one-dimensional photonic crystal formed by the layered system (see figure 1). We choose the z-axis to be normal to the interface, the x-axis to be in the plane of the figure, and the y-axis to be out of the plane of the figure. While our arguments will apply to a wave with arbitrary polarization, we have considered the p-polarization mode without any loss of generality, since, at normal incidence, both s- and p-polarizations give the same results.

The isotropic electromagnetic medium can generally be described by a dielectric permittivity ϵ and magnetic permeability μ. Its dispersion relation can be obtained by solving the wave equation [19, 27]:

$$-\frac{Z(x)}{n(x)}\frac{\mathrm{d}}{\mathrm{d}x}\left[\frac{1}{Z(x)n(x)}\frac{\mathrm{d}E(x)}{\mathrm{d}x}\right]=\left(\frac{\omega}{c}\right)^2 E(x), \tag{1}$$

where $n(x) = \sqrt{\epsilon(x)}\sqrt{\mu(x)}$ and $Z(x) = \sqrt{\mu(x)}/\sqrt{\epsilon(x)}$ are the refractive index and the impedance at frequency ω, respectively. They are layer dependent. The medium A, with thickness d_A, is fulfilled by SiO_2 and is characterized by a constant positive refractive index n_A. The medium B, with thickness d_B, is fulfilled by a metamaterial, characterized by a negative refractive index $n_B = \sqrt{\epsilon_B}\sqrt{\mu_B}$. They are surrounded by the transparent medium C with a constant refractive index n_C (see figure 1).

In order to obtain the transmission spectra, we must relate the amplitudes A^0_{1C} and A^0_{2C} of the electromagnetic field in the transparent medium C at $z < 0$ to those in the region $z > L$, where L is the size of the quasiperiodic structure, by successive applications of the above equation in each layer, together with Maxwell's electromagnetic boundary conditions at each interface along the multilayer system.

The transmission of a normal incident light wave across the interfaces $\alpha \to \beta$ (α, β being any A, B and C medium) is defined by the interface matrices

$$M_{\alpha\beta} = \frac{1}{2}\begin{pmatrix} 1 + Z_\alpha/Z_\beta & 1 - Z_\alpha/Z_\beta \\ 1 - Z_\alpha/Z_\beta & 1 + Z_\alpha/Z_\beta \end{pmatrix}. \tag{2}$$

The propagation of the light wave within one of the layers γ ($\gamma = A$ or B) is characterized by the propagation matrices

$$M_\gamma = \begin{pmatrix} \exp(-\mathrm{i}k_\gamma d_\gamma) & 0 \\ 0 & \exp(\mathrm{i}k_\gamma d_\gamma) \end{pmatrix}, \tag{3}$$

with $k_\gamma = n_\gamma \omega/c$.

For the whole quasiperiodic structure, we obtain

$$\begin{pmatrix} A^0_{1C} \\ A^0_{2C} \end{pmatrix} = M_N \begin{pmatrix} A^m_{1C} \\ 0 \end{pmatrix}, \tag{4}$$

with $M_N = M_{CA}M_A M_{AB} M_B M_{BA} M_A \cdots M_{BC}$, being the optical transfer matrix of the Nth-generation quasiperiodic multilayer system. This relates the amplitudes A^0_{1C} and A^0_{2C} of the electromagnetic field in the transparent medium C at $z < 0$ to those in the region $z > L$, where L is the size of the quasiperiodic structure. This transfer matrix is formed by the product of matrices $M_{\alpha\beta}$ ($\alpha, \beta = A, B$ or C) and M_γ ($\gamma = A$ or B) according to the type of quasiperiodic array and the generation number N of the quasiperiodic sequence considered in the multilayer arrangement.

The reflectance and the transmittance coefficients are simply given by

$$R = \left|\frac{M_{21}}{M_{11}}\right|^2 \qquad \text{and} \qquad T = \left|\frac{1}{M_{11}}\right|^2, \tag{5}$$

where $M_{i,j}$ ($i, j = 1, 2$) are the elements of the optical transfer matrix M_N.

3. Numerical results

In this section we present numerical simulations for light transmission through the quasiperiodic multilayered photonic structure. Let us first assume an ideal model system in which both the magnetic permeability and the electric permittivity can be approximated by constants in the frequency range of interest. We have chosen medium A as silicon dioxide (SiO_2), whose refraction index is $n_A = 1.45$, while medium B is considered to have

$n_B = -1$. Also, we assume the individual layers to be quarter-wave layers, for which the quasiperiodicity is expected to be more effective [28], with the central wavelength $\lambda_0 = 700$ nm. These conditions yield the physical thickness $d_J = (175/n_J)$ nm, $J = A$ or B, such that $n_A d_A = n_B d_B$, which gives a very reversed phase shift in the two materials. Defining $\bar{n} = n_A d_A + n_B d_B$, this assumption means the so-called zero-$\bar{n}$ photonic region. Further, we also consider medium C to be a vacuum, and the phase shifts are given by:

$$\delta_A = (\pi/2)\Omega\cos(\theta_A); \qquad \delta_B = -(\pi/2)\Omega\cos(\theta_B) \tag{6}$$

where Ω is the reduced frequency $\Omega = \omega/\omega_0 = \lambda_0/\lambda$.

For normal incidence, $\theta_A = \theta_B = 0$, and $\delta_A = -\delta_B$. Here, the negative phase shift for medium B means that the light waves propagate in a direction opposite to the energy flux ($+z$-direction in figure 1), i.e. one plane light wave, whose electromagnetic field is proportional to $\exp(-i\delta_B)$, will itself propagate in the ($-z$)-direction, while the Poynting vector propagates in the ($+z$)-direction. Therefore, at medium B the effect of the negative refraction index is to change the forward waves $\exp(i\delta_B)$ into backward waves $\exp(-i\delta_B)$ and vice versa. This effect keeps the same configuration for the incident and reflected electromagnetic wave at the interface A–B, but the electromagnetic wave at layer B has a sign change in the exponentials when compared to the electromagnetic wave at layer A. This effect is expected to be reflected somehow in the transmission spectra of the quasiperiodic multilayered systems treated here.

The optical transmission spectrum for the ninth-generation (55-layer) quasiperiodic Fibonacci sequence, as a function of the reduced frequency Ω, is shown in figure 2(a). The transmission spectrum presents a unique mirror symmetrical profile around the midgap frequency $\Omega = 1$ (which is, of course, the midgap frequency of a periodic quarter-wavelength multilayer). Besides, the structure is transparent (the transmission coefficient is closely equal to 1.0) at the reduced frequencies $\Omega = 0.898$ and $\Omega = 1.101$, as we can see in figure 2(b), forming two broad peaks, also distributed symmetrically around $\Omega = 1$. The condition of transparentness implies that the layers A and B are equivalent from a wave point of view. Furthermore, the transmission spectrum has a scaling property with respect to the generation number of the Fibonacci sequence, within a symmetrical interval around $\Omega = 1$. To understand this scaling property, consider figure 2(b), which shows the optical transmission spectrum of figure 2(a) for the range $0.80 < \Omega < 1.20$. This spectrum is the same, as shown in figure 2(c), to the one representing the fifteenth-generation (877-layer) quasiperiodic Fibonacci sequence (i.e. it has been recovered after six Fibonacci generations), for the range of frequency reduced by a scale factor approximately equal to 25. Although it has a different scale and profile, as expected, this striking self-similar pattern was also found for the case where medium B is a positive refractive index material [24], and indeed this is a consequence that all Fibonacci structures possess a self-similarity profile around the fixed point $\delta = (m + 1/2)\pi$, $m = 0, 1, \ldots$ [29].

The spectrum for the Thue–Morse quasiperiodic structure for its ninth generation is shown in figure 3. The transmission spectrum again presents a unique mirror symmetrical profile around the midgap frequency $\Omega = 1$. However, instead of exhibiting a self-similar transmission coefficient, as observed for the Fibonacci case, the numerical solution shows that the photonic band gap covers all frequencies, except for the singular frequency points $\Omega = 0, 1, 2, \ldots$, meaning delta shifts equal to integral multiples of $\pi/2$. This fact is in apparent disagreement with the result presented in [19], where the photonic gap, considering a periodic stack $ABAB\cdots$, was found to cover all frequencies except for singular frequency points with delta shifts equal to integral multiples of π. However, for large-generation numbers (the transverse magnetic, or TM, ninth generation number means 2^{10} building blocks A and B), the Thue–Morse quasiperiodic structure resembles the periodic $AABBAABB\cdots$ array

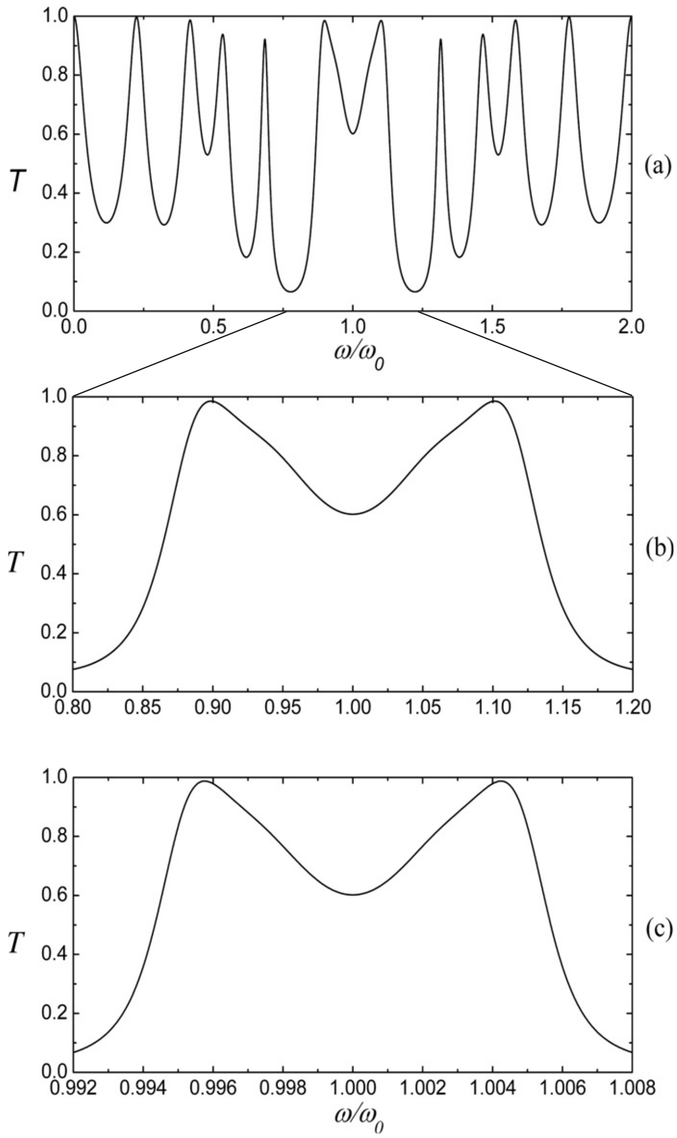

Figure 2. Normal-incidence transmission spectra of light beam into a quasiperiodic Fibonacci multilayered photonic structure: (a) the transmittance T as a function of the reduced frequency $\Omega = \omega/\omega_0$ for the ninth generation of the Fibonacci sequence; (b) same as in (a), but for the reduced range of frequency $0.8 \leqslant \Omega \leqslant 1.2$; (c) same as in (b), but for the 15th generation of the Fibonacci sequence.

(although they are not totally equal to each other), leading to delta shifts equal to integral multiples of $\pi/2$ instead of π, notwithstanding the fact that the magnitude of the transmissions depicted in figure 3 is, as expected, not exactly equal to one, as for the one presented in [19]. Note that this spectrum is very different from those shown in [24] for the same sequence, but for positive refractive index.

The optical transmission spectrum for the ninth-generation double-period quasiperiodic structure is depicted in figure 4. The structure is symmetrically distributed around $\Omega = 1$,

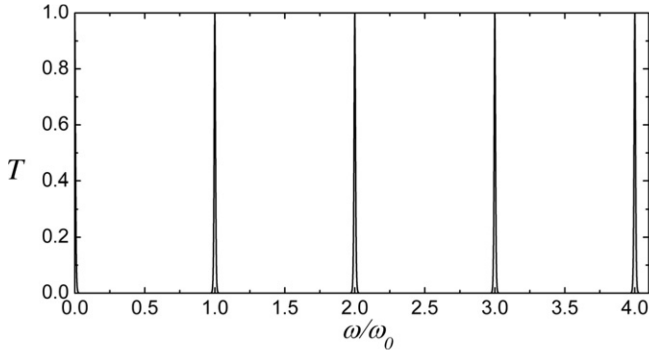

Figure 3. The normal-incident transmission spectra as a function of the reduced frequency $\Omega = \omega/\omega_0$ for the ninth generation of the Thue-Morse sequence.

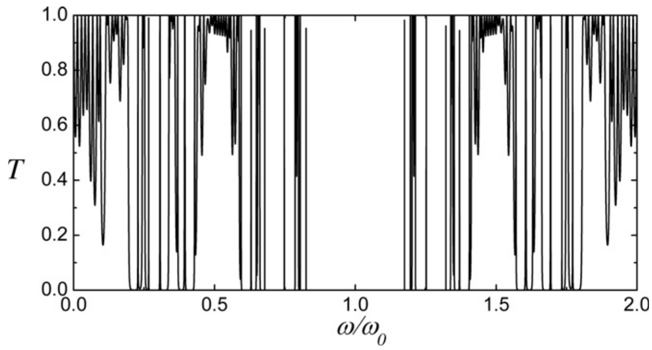

Figure 4. As in figure 3, but for the ninth generation of the double-period sequence.

and shows photonic band gaps, the biggest one for the range of the reduced frequency $0.8 < \Omega < 1.20$. The presence of such a large band gap in the central frequency range area is a surprising result, and has no counterpart either with the other quasiperiodic sequences studied here or with those obtained for a multilayered system without the presence of a metamaterial.

The influence of the metamaterial in the light wave transmission spectra in the quasiperiodic superlattices is shown in figure 5 by means of the transmission rate as a function of the negative refraction index n in layer B, considering the midgap frequency of a periodic quarter-wavelength multilayer $\Omega = 1$. The Fibonacci case is plotted in figure 5(a), while the Thue–Morse and double-period cases are plotted in figures 5(b) and (c), respectively. We have considered all of them represented by their ninth generation. Quite interestingly, we can now observe that the optical transmission spectra for all sequences presents a different oscillatory behaviour for each quasiperiodic structure. For the Fibonacci and double-period cases, the structure is periodic within the interval $2m - 1 < |n| < 2m + 1$, $m = 1, 2, \ldots$, while for the Thue–Morse case the periodicity is defined within the range $m < |n| < 2m$, $m = 1, 2, \ldots$. There is a narrow band gap for the double-period case around the odd values of the refractive index, with no counterpart for the other quasiperiodic structures.

The above discussions apply only to the ideal case where both the magnetic permeability and the electrical permittivity are frequency non-dispersive, which is valid under the assumption that the size of the fabricated negative refractive index material can be as tiny as the normal positive refractive index material. However, all realized artificial negative refractive index

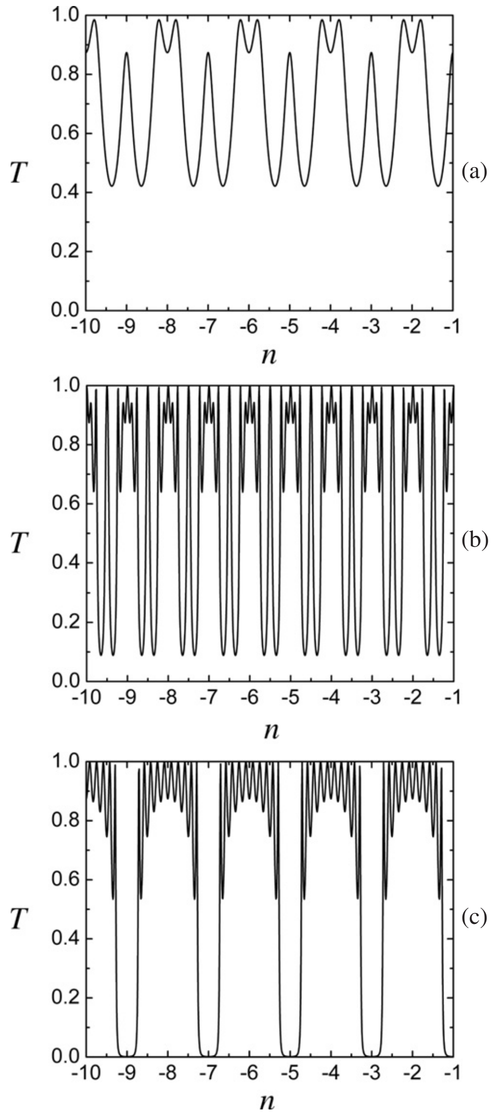

Figure 5. Transmission coefficients T as a function of the absolute value of the negative refraction index n at $\Omega = \omega/\omega_0 = 1$. We have considered the ninth generation for all quasiperiodic structures: (a) Fibonacci; (b) Thue–Morse; (c) double-period.

metamaterials have an electric permittivity ϵ and a magnetic permeability μ that are frequency dispersive, being simultaneously negative only within a narrow frequency bandwidth. Since microstructures of practical negative refractive metamaterials are of the order of a few millimetres, their typical frequency region ranges from 1 to 14 GHz.

For convenience, we will use a causal plasmonic form for the dielectric permittivity $\epsilon(\omega)$ mimicking the Drude–Lorentz model, which can be achieved by using an array of wire elements into which cuts are periodically introduced. Neglecting any damping term (when lossy metamaterial is considered, the dumping factor can be defined as a fraction of the plasma frequency), the composite material possesses a negative refractive index in the microwave region, whose corresponding dielectric permittivity $\epsilon(\omega)$ and magnetic permeability $\mu(\omega)$ are

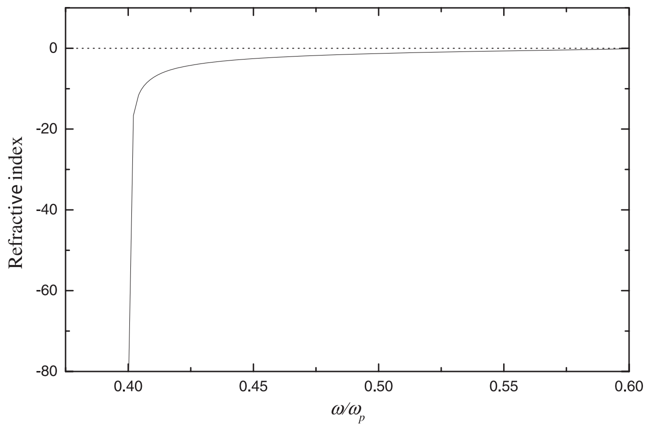

Figure 6. Profile of the negative refractive index in layer B (metamaterial) as a function of the reduced frequency $\omega/\omega_{\rm p}$, where $\omega_{\rm p}$ is the plasma frequency.

given respectively by [30]:

$$\epsilon(\omega) = 1 - \omega_{\rm p}^2/\omega^2, \tag{7}$$

$$\mu(\omega) = 1 - F\omega^2/(\omega^2 - \omega_0^2), \tag{8}$$

where the plasma frequency $\omega_{\rm p}$, the resonance frequency ω_0, and the fraction F are determined only by the geometry of the lattice rather than by the charge, effective mass and density of electrons, as is the case in naturally occurring materials. In this work we use $\omega_0/2\pi = 4$ GHz, $\omega_{\rm p}/2\pi = 10$ GHz, and $F = 0.56$, motivated by the experimental work of Smith and collaborators [4].

Figure 6 shows the profile of the refractive index in the metamaterial layer (B) as a function of the reduced frequency $\omega/\omega_{\rm p}$, corresponding to the range of frequency from 4 to 6 GHz, where the permittivity and the permeability are simultaneously negative. Observe the sharp behaviour of the negative refractive index near the frequency close to 4 GHz. Then, it shows a smooth profile until it reaches a 6 GHz frequency which defines the frequency region for the zero refractive index. This zero refractive index displays a narrow spectral gap in transmission, which is quite different from the usual Bragg reflected band gap. For frequencies larger than 6 GHz, both the metamaterial and SiO_2 have a positive refractive index n. Therefore the band gaps above this frequency result from the Bragg reflection due to the modulation of the impedance and the refractive index.

In figure 7 we show the transmission spectra for the quasiperiodic sequences studied here, considering the refractive index n_B depending on ω in the frequency range $0.4 < \omega/\omega_{\rm p} < 0.6$, where it is negative (see figure 6). The thickness of each medium is chosen from $(\epsilon_{j\infty})^{1/2}d_j = \lambda_0/4$, with $\epsilon_{A\infty} = \epsilon_A = 12.3$, $\mu_A(\omega) = 1$ and $\epsilon_{B\infty} = 1$. In figure 7(a) we show the transmission spectra for the Fibonacci sequence considering its generation number $N = 5, 6, 7, 8$. Clearly, we can observe that the spectra is no longer self-similar. Furthermore, instead of a symmetrical distribution, we have an optical gap, starting from $\omega = 0.425$, which becomes broader as long as the Fibonacci generation number N increases. After that, it presents several Bragg peaks, whose number also increases with N. The transmission spectra for the Thue–Morse quasiperiodic multilayered structure is plotted in figure 7(b) for its generation number $N = 5, 6, 7, 8$. Again, we can observe a symmetry-break also for this case and an optical main gap in the range $0.465 < \omega/\omega_{\rm p} < 0.485$. For the double-period case, depicted in figure 7(c), the transmission spectra are more similar to the Fibonacci case, but

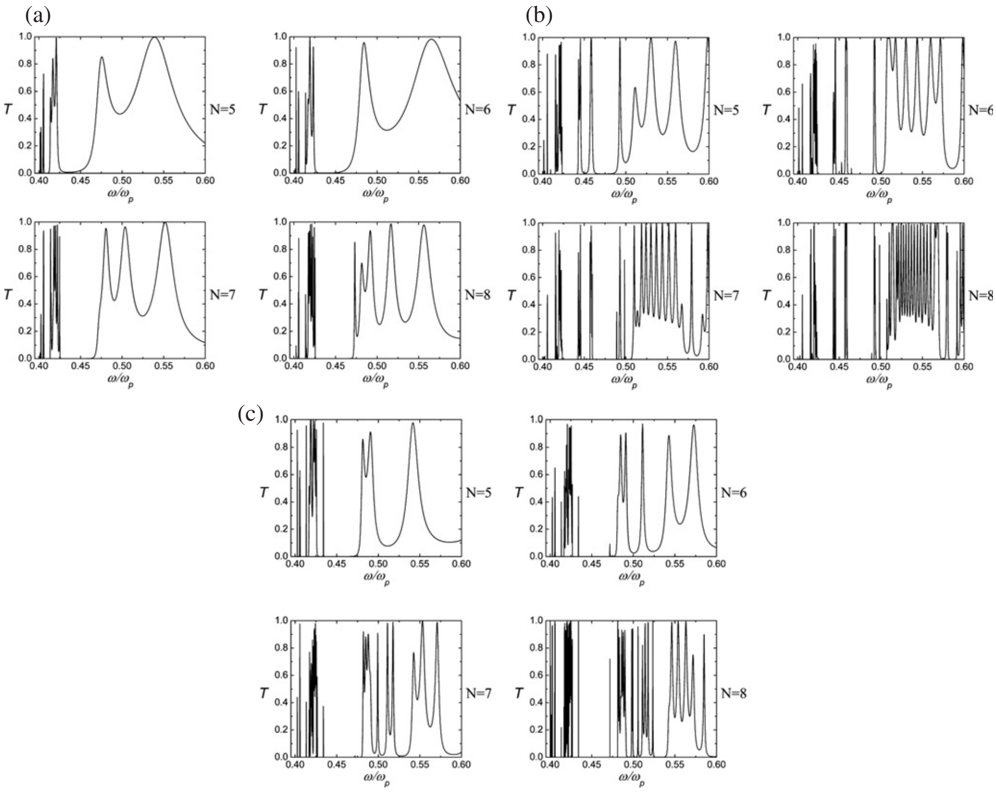

Figure 7. Transmission coefficients T as a function of the reduced frequency ω/ω_p for the case of normal incidence, considering different generation numbers of the quasiperiodic structures: (a) Fibonacci; (b) Thue–Morse; (c) douple-period.

with a richer structure of Bragg peaks, together with a broader pass-band around $\omega/\omega_\mathrm{p} = 0.45$. Also, observe the formation of another broad peak around $\omega/\omega_\mathrm{p} = 0.53$ as the double-period generation number increases.

4. Conclusions

In summary, we have presented the transmission spectra of light waves which propagate through quasiperiodic Fibonacci, Thue–Morse and double-period multilayers, where one of their components has a negative refractive index. Considering a frequency-independent refractive index, a striking self-similar pattern is presented for the Fibonacci structure. Furthermore, a unique mirror symmetric profile, with no counterpart for the positive refractive index case, is the main signature of the light transmission spectra in all the quasiperiodic structures considered here. On the other hand, a more realistic frequency-dependent refractive index for the metamaterial layer B gives rise to a rich transmission profile of Bragg peaks with no more self-similarity or mirror symmetry in their optical transmission spectra.

Acknowledgments

We would like to thank partial financial support from the Brazilian Research Agencies CNPq-Edital Universal, CNPq-Rede Nanobioestruturas, FINEP-CTInfra, and FAPEMA. One of us

(ELA) also thanks a Capes-Fulbright scholarship at the Center for Polymer Studies, Boston University, in Boston, MA, USA.

References

[1] Veselago V G 1968 *Sov. Phys.—Usp.* **10** 509
[2] Ramakrishna S A 2005 *Rep. Prog. Phys.* **68** 449
[3] Pendry J B, Holden A, Robbins D J and Stewart W J 1999 *IEEE Trans. Microw. Theory Tech.* **47** 2075
[4] Smith D R, Padilla W J, Vier D C, Nemat-Nasser S C and Schultz S 2000 *Phys. Rev. Lett.* **84** 4184
[5] Shelby R A, Smith D R and Shultz S 2001 *Science* **292** 77
[6] Parimi P V, Lu W T, Vodo P and Sridhar S 2003 *Nature* **426** 404
[7] Pendry J B 2000 *Phys. Rev. Lett.* **85** 3966
[8] Smith D R, Pendry J B and Wiltshire M C K 2004 *Science* **305** 788
[9] Parazzoli C G, Greegor R B, Li K, Koltenbah B E and Tanielian M 2003 *Phys. Rev. Lett.* **90** 107401
[10] Pendry J B 2004 *Science* **306** 1353
[11] Houck A, Brock J B and Chuang I L 2003 *Phys. Rev. Lett.* **90** 137401
[12] Notomi M 2000 *Phys. Rev.* B **62** 1069
[13] Foteinopoulou S and Soukoulis C M 2003 *Phys. Rev. Lett.* **90** 107402
[14] Cubukcu E, Aydin K, Ozbay E, Foteinopoulou S and Soukoulis C M 2003 *Nature* **423** 604
[15] Wang X, Ren Z F and Kempa K 2004 *Opt. Express* **12** 2919
[16] Shalaev V M, Cai W, Chettiar U K, Yuan H-K, Sarychev A K, Drachev V P and Kildishev A V 2005 *Opt. Lett.* **30** 3356
[17] Drachev V P, Cai W, Chettiar U K, Yuan H-K, Sarychev A K, Kildishev A V, Klimeck G and Shalaev V M 2005 *Opt. Lett.* **30** 3356
[18] Zhang Z M and Fu C J 2001 *Appl. Phys. Lett.* **80** 1097
[19] Li J, Zhou L, Chan C T and Sheng P 2003 *Phys. Rev. Lett.* **90** 083901
[20] Albuquerque E L and Cottam M G 2004 *Polaritons in Periodic and Quasiperiodic Structures* (Amsterdam: Elsevier)
[21] Zhu S N, Zhu Y Y, Qin Y Q, Wang H F, Ge C Z and Ming N B 1997 *Phys. Rev. Lett.* **78** 2752
[22] Zhu S N, Zhu Y Y and Ming N B 1997 *Science* **27** 8843
[23] Zhang X, Zhang Z-Q and Chan C T 2001 *Phys. Rev.* B **63** 081105
[24] Vasconcelos M S, Albuquerque E L and Mariz A M 1998 *J. Phys.: Condens. Matter* **10** 5839
[25] Vasconcelos M S and Albuquerque E L 1999 *Phys. Rev.* B **59** 11128
[26] Albuquerque E L and Cottam M G 2003 *Phys. Rep.* **376** 225
[27] Zhang Z-Q 1995 *Phys. Rev.* B **52** 7960
[28] Kono K, Nakada S, Narahara Y and Ootuka Y 1991 *J. Phys. Soc. Japan* **60** 368
[29] Kohmoto M, Sutherland B and Iguchi K 1987 *Phys. Rev. Lett.* **58** 2436
[30] Shadrivov H V, Sukhorukov A A and Kivshar Y S 2003 *Appl. Phys. Lett.* **82** 3820